Journal of Power Sources 218 (2012) 187–191

Contents lists available at SciVerse ScienceDirect

Journal of Power Sources

journal homepage: www.elsevier.com/locate/jpowsour

Thickness effects of yttria-doped ceria interlayers on solid oxide fuel cells

Zeng Fan [a,*], Jihwan An [b], Andrei Iancu [b], Fritz B. Prinz [a,b]

[a] Department of Materials Science and Engineering, Stanford University, Stanford, CA 94305, USA
[b] Department of Mechanical Engineering, Stanford University, Stanford, CA 94305, USA

HIGHLIGHTS

- Yttria-doped ceria interlayers are fabricated by atomic layer deposition.
- The completeness of YDC films with various ALD super cycles is studied through electroanalysis.
- Auger elemental mapping and X-ray photoelectron spectroscopy are used to verify the film coverage.
- The effect of the optimal YDC interlayer in micro fuel cells is presented.

GRAPHICAL ABSTRACT

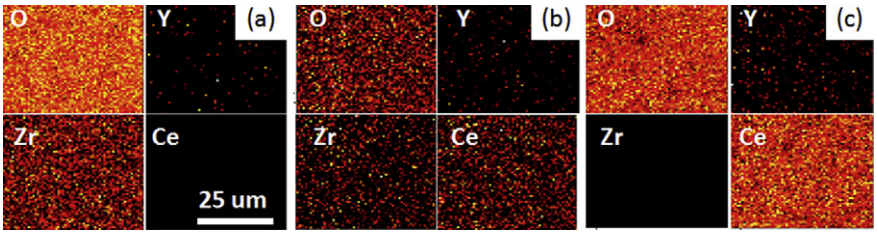

ARTICLE INFO

Article history:
Received 20 March 2012
Received in revised form
27 June 2012
Accepted 30 June 2012
Available online 7 July 2012

Keywords:
Yttria-doped ceria
Atomic layer deposition
Interlayer
Thickness effects
Low temperature solid oxide fuel cell

ABSTRACT

Determining the optimal thickness range of the interlayed yttria-doped ceria (YDC) films promises to further enhance the performance of solid oxide fuel cells (SOFCs) at low operating temperatures. The YDC interlayers are fabricated by the atomic layer deposition (ALD) method with one super cycle of the YDC deposition consisting of 6 ceria deposition cycles and one yttria deposition cycle. YDC films of various numbers of ALD super cycles, ranging from 2 to 35, are interlayered into bulk fuel cells with a 200 um thick yttria-stabilized zirconia (YSZ) electrolyte. Measurements and analysis of the linear sweep voltammetry of these fuel cells reveal that the performance of the given cells is maximized at 10 super cycles. Auger elemental mapping and X-ray photoelectron spectroscopy (XPS) techniques are employed to determine the film completeness, and they verify 10 super cycles of YDC to be the critical thickness point. This optimal YDC interlayer condition (6Ce1Y × 10 super cycles) is applied to the case of micro fuel cells as well, and the average performance enhancement factor is 1.4 at operating temperatures of 400 and 450 °C. A power density of 1.04 W cm^{-2} at 500 °C is also achieved with the optimal YDC recipe.

1. Introduction

Fuel cells are conversion devices that transform chemical energy of fuel into electrical energy [1,2]. Solid oxide fuel cells (SOFC) with ceramic electrolyte membranes represent a major class of fuel cells. Yttria stabilized zirconia (YSZ) has been commonly used as the electrolyte material for its high stability and decent ionic conductivity [2–4]. Because of fuel flexibility and high efficiency, SOFCs are especially attractive for stationary applications. However, SOFCs have to operate at high temperatures (>600 °C) to maintain sufficient power output. This temperature limitation is mainly due to two factors: the reduced ionic conductivity of the electrolyte material and the sluggish oxide ion incorporation kinetics at the electrode/electrolyte interface at relatively low operating temperatures (<600 °C) [5–7]. In recent years, several studies have focused on addressing the above two factors, including our recent work that utilized the yttria-doped ceria (YDC) interlayer to enhance the power density of the given SOFCs [8–14]. Our results showed that this added thin film (≈17.5 nm) effectively reduced the cathode/interfacial activation energy by 0.1 eV and increased the exchange current density by a factor of 4 at operating temperatures between 300 and 500 °C. As a result, the cell

* Corresponding author.
E-mail address: fanzeng@stanford.edu (Z. Fan).

0378-7753/$ – see front matter © 2012 Elsevier B.V. All rights reserved.
http://dx.doi.org/10.1016/j.jpowsour.2012.06.103

performance can be enhanced by about three times at such low operating temperatures. Based on the previous findings, the ALD recipe for the YDC deposition is fixed as Ce: $Y = 6$: 1 in this paper, meaning one ALD super cycle of the YDC deposition consists of 6 ceria deposition cycles and one yttria deposition cycle. For this study, we aimed to examine the growth conditions of YDC thin films, and to further enhance the power densities of low-temperature SOFCs by identifying the minimal number of YDC super cycles needed to form a complete film.

Atomic layer deposition (ALD) is well known for its precise-layer control and uniformity of the deposited films [15,16]. Our lab has successfully grown high-quality YDC films by ALD and has been able to precisely control the stoichiometry and thickness of these films [13]. The YDC films discussed in this paper were all deposited by the ALD method. In the ALD growth mechanism, as the number of ALD cycles increases, the deposition process starts from island growth on the substrate to gradually form a complete film one sub-monolayer at a time [17,18]. Since the oxide ion incorporation is faster at the YDC–Pt interface than YSZ–Pt interface, we want to guarantee that YDC films have fully covered the underlying YSZ electrolyte [13]. However, once the YDC film is complete, the additional increment in the film thickness will cause unnecessary ohmic resistance. This extra ohmic loss may seem negligible for fuel cells with a bulk YSZ (200 um) electrolyte; however, it can cause significant performance loss for micro fuel cells with an electrolyte thinner than 100 nm. Therefore, studying ALD growth conditions of the interlayered YDC films and determining their critical thickness range are important to maximizing the fuel cell performance operating at comparatively low temperatures. In this study, we performed *I–V* measurements on the interlayered fuel cells with various numbers of YDC super cycles to identify the critical numbers of these cycles that correspond to the maximum power densitsies and then used Auger elemental mapping and X-ray photoelectron spectroscopy (XPS) techniques to analyze the completeness of the film coverage. Last, we demonstrated how to apply the optimal ALD-YDC layer to micro fuel cells and how, as a result, a record high power density can be achieved under the desired working conditions.

2. Methods

Fabrication of YDC thin film interlayers was done by the ALD method. Commercially available tris(methylcyclopentadienyl)-yttrium (III) (99.9% purity, Strem Chemicals) and Tetrakis (2,2,6,6-tetramethyl-3,5-heptanedionato)-cerium(IV) (min. 97% purity, Strem Chemicals) were used as Y_2O_3 and CeO_2 precursors, respectively. Ozone was utilized as the oxidant source. A detailed description of our ALD process was published in a previous paper [13]. In this study, we fixed the recipe of one super cycle of the YDC deposition at a pulsing ratio of 6 Ce: 1 Y, which yields the deposited film with a stoichiometry of 14 M % of yttria and has been proved to be the optimal doping level for the oxide ion incorporation into the given YDC interlayer. In order to study the thickness effects, we varied the number of YDC super cycles as 2, 5, 10, 15, 20, and 35. These YDC films with various thicknesses were directly deposited onto the cathode side of the cleaned YSZ substrates (polycrystalline, Φ 17 mm×200 um, 8 M % yttria concentration, double-side polished, BEANS International Corporation). Porous Pt with a size of 0.5 cm^2 was then sputtered and employed as both cathode and anode.

Reference samples were SOFCs without the addition of the YDC interlayer; their fabrication process was detailed in another paper from our lab [13]. The linear sweep voltammery method was used to measure the performance of reference fuel cells and fuel cells interlayered with various YDC thicknesses. All the cells were kept in a sealed test chamber to maintain the constant operating temperature, and were measured at 300–450 °C. 15 sccm dry H_2 was supplied to the anode side of the cells and air on the cathode side. A Gamry Potentiostat (FAS2, Germany Instruments, Inc) unit was used to collect current–voltage (*I–V*) data. By comparing the maximum power densities across fuel cells with different number of super cycles of the deposited YDC interlayers, we identified 10 super cycles as the critical cycle number; YDC interlayers with more than 10 super cycles did not yield additional performance enhancement.

To verify that the minimum number of super cycles needed to achieve full surface coverage with the YDC film is 10, we employed Auger elemental mapping and X-ray photoelectron spectroscopy (XPS) techniques. For the Auger analysis (PHI 700 Scanning Auger Nanoprobe), we performed elemental mapping (O, Y, Zr and Ce) on three samples: a reference sample, an YSZ substrate with 5 super cycles of YDC and an YSZ substrate with 10 super cycles of YDC. Due to the highly insulating nature of the materials, several steps were taken to minimize charging including: completely wrapping the sample in aluminum foil, analyzing the sample through a very small hole in the aluminum foil, using a low energy electron beam for additional neutralization and slightly defocusing the primary electron beam to increase its spot size on the sample. Using these techniques, charging effects were effectively minimized and the signal to noise ratio was significantly improved to provide repeatable, high quality elemental data. By observing the bright spot intensities transitioning gradually from Zr to Ce in the mapping images, we visualized the YDC coverage process and identified that the YDC film of 10 super cycles was complete and fully covered the underlying YSZ substrate. For the XPS analysis (PHI Versa Probe 5000, Physical Electronics, USA), three samples with different YDC interlayering conditions, 5, 10 and 15 super cycles of YDC (6Ce: 1Y), were examined. If the YDC film was complete, no Zr-3d peak from the underlying YSZ substrate would be discernible through the XPS surface scan. By comparing Zr-3d peaks of the above three samples, we also learned that 10 super cycles of YDC was enough to form a complete film. Both the XPS and Auger results helped to confirm that the optimal ALD recipe for the YDC interlayer is (6Ce: 1Y) × 10 in terms of thickness.

When the electrolyte thickness of a SOFC is reduced to sub-100 nm range, the thickness of the interlayered YDC becomes more critical. The minimum needed thickness of the YDC interlayer

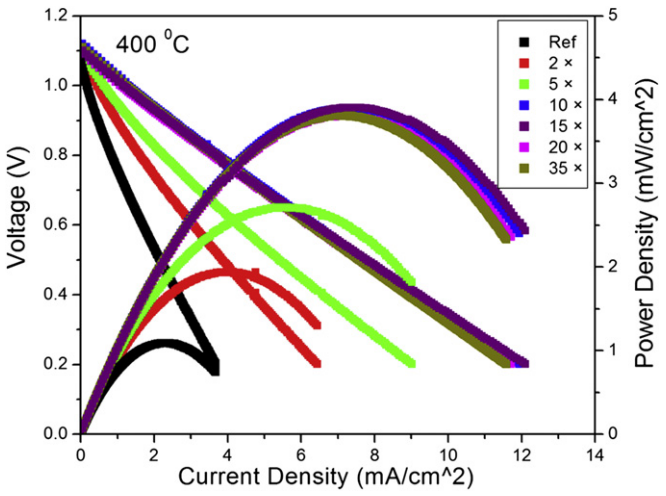

Fig. 1. Current density vs. voltage and power density of SOFCs with different YDC interlayers on polycrystalline YSZ substrates operated at 400 °C. The plot shows gradual performance enhancement up to 10 super cycles of YDC, beyond which no additional cell performance enhancement is observed.

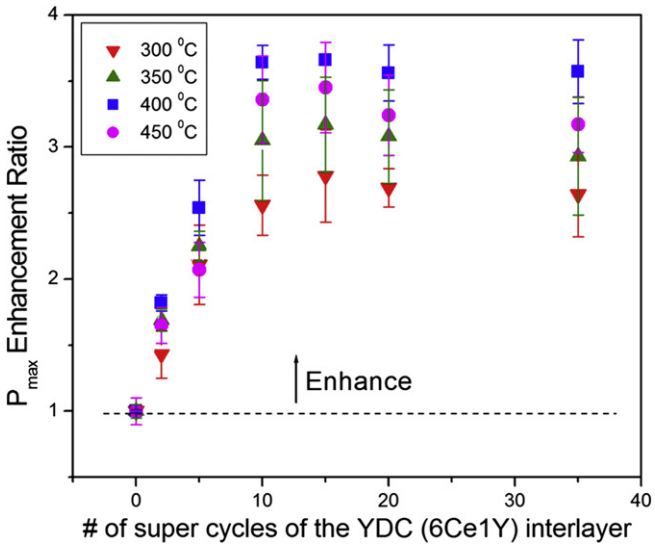

Fig. 2. Maximum power density enhancement ratio as a function of # of ALD super cycles and operating temperature for SOFCs with polycrystalline YSZ substrates. The YDC interlayers were deposited by the same stoichiometric ratio Ce: $Y = 6$: 1. Reference SOFC samples without YDC interlayering are indicated as 0 super cycles.

should be adopted to avoid unnecessary ohmic loss. Based on this rationale, we deposited the YDC interlayer with the identified optimal recipe (6 Ce: 1Y×10) and applied this film to micro fuel cells, whose fabrication process has been described by Huang [19]. YSZ was employed as the fuel cell electrolyte and was also deposited by ALD. The YSZ film was 70 nm thick and had an 8 M % of Y_2O_3 doping level. A Si_3N_4 buffer layer was patterned and removed by reactive ion etching (RIE). The exposed Si area was subject to 30% KOH etching, and, as a result, micro-sized windows were developed. Here, Scanning Electron Microscopy (SEM) was employed to verify the window size. After this step, the optimal YDC interlayer (6Ce: 1Y × 10) was deposited onto the freestanding YSZ. Last, 80 nm thick porous Pt was sputtered onto the fuel cells acting as both cathode and anode. The whole fabricated wafer (4″) was cut into 1 cm × 1 cm chips and was ready for performance testing. Each testing chip was placed into a customized test station, and a microprobe manipulator was used to select the individual fuel cell to measure. The anode side of the cells was sealed and received a constant supply of 20 sccm dry H_2, while the cathode was open to the air. The same Gamry (Gamry/FAS-32) unit was employed to conduct *I–V* measurements for micro fuel cells with and without the optimal YDC interlayer at 400 and 450 °C. During the measurements, a temperature controller was used to maintain the constant station temperature.

3. Results and discussion

Reference SOFCs and fuel cells with various cycles of YDC interlayering were tested at operating temperatures between 300 and 450 °C. *I–V* data were collected by Gamry and were used to calculate the corresponding power densities. Fig. 1 shows the *I–V* and *I–P* curves for these cells at 400 °C. Since the Y_2O_3 doping level was fixed at 14 M% in all interlayered samples, the performance difference was due only to the thickness effects of the deposited YDC films. As expected, once the YDC interlayer was added between the YSZ electrolyte and Pt, the activation loss of the given cell was significantly reduced due to the enhanced interfacial kinetics at the Pt–YDC interface. The maximum power density (P_{max}) of the given cell, at the same time, was increased as well. This phenomenon was obvious after introducing only 2 super cycles of YDC. As the number of YDC super cycles increased, P_{max} was enhanced even more. However, P_{max} started to saturate once YDC reached 10 super cycles, suggesting a complete ALD film started to form from there. This hypothesis was further strengthened by the fact that additional super cycles beyond 10 did not yield better fuel cell performance. 10 ALD super cycles grow a 6–7 nm thick YDC film, therefore, the critical thickness for full coverage is 6–7 nm [13]. We define the quotient of the YDC interlayered sample's P_{max} to the reference YSZ sample's P_{max} as the P_{max} enhancement ratio. In Fig. 2, this ratio is plotted as a function of the number of ALD super cycles of YDC under different operating temperatures. The zero super cycle represents reference SOFCs without YDC interlayering, which had P_{max} of 0.064, 0.325, 1.07 and 3.44 mW cm^{-2} at 300, 350, 400 and 450 °C, respectively. Since all the YDC interlayers were deposited with the optimal doping level as 14 M %, the inserted YDC layers, regardless of thickness, all helped to enhance the fuel cell performance. Starting from 10 YDC super cycles, a P_{max} enhancement ratio of 2.5–3.7 was achieved under the experimental conditions, indicating the optimal ALD recipe is (6Ce: 1Y) × 10. This YDC interlayer with the optimal ALD recipe can also be applied to SOFCs with other electrode materials besides Pt, and the performance of those fuel cells is expected to be enhanced in a similar fashion.

In order to verify that (6Ce: 1Y) × 10 is the optimal ALD recipe for interlayered YDC films, we conducted Auger elemental mapping on the reference SOFCs and on SOFCs with various YDC super cycles. Fig. 3 shows normalized atomic percentage maps for

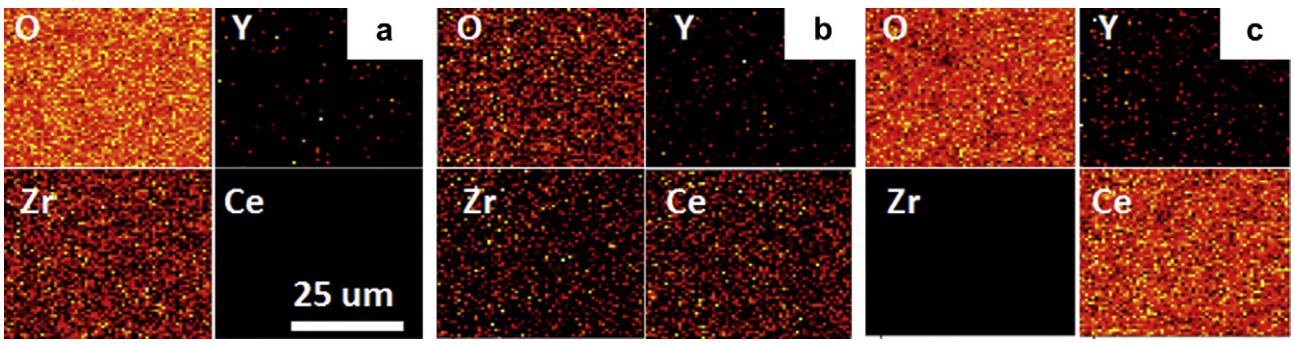

Fig. 3. Auger elemental mapping on surfaces of 3 samples. These are normalized atomic percentage maps for a 50 um by 50 um region of each surface. (a) Mapping on bare YSZ surface. There is a great amount of Zr and O on the surface while there is no Ce; Y bright spots sprinkled randomly as well. (b) 5 super cycles of YDC on top of the YSZ substrate. Ce shows strong intensity while Zr is significantly weakened, indicating that the YSZ surface was partially covered by YDC. (c) 10 super cycles of YDC on top of the YSZ substrate. Zr totally disappears while a significant amount of Ce is detected on the surface. O and Y relatively are unchanged. This image shows the total coverage of YDC on YSZ.

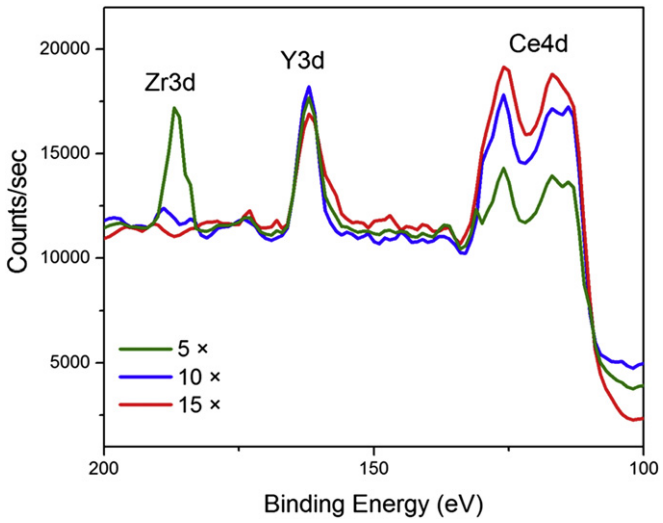

Fig. 4. Surface sensitive XPS analysis of three YDC interlayered SOFCs between 100 and 200 eV Zr3d, Y3d and Ce4d peaks are all within this binding energy regime. A 10 eV neutralizer was turned on to avoid surface charging effects.

a 50 um × 50 um region of the given surfaces. The relative elemental concentration is represented by the intensity of the bright dots in the map. As expected, for the reference sample, Zr had a high intensity, while none of the Ce was observed because the surface was pure YSZ. In contrast, for SOFCs coated with 5 super cycles of YDC, the Zr intensity was weakened while Ce displayed much stronger signals. When YDC super cycles increased to 10, Ce totally took over Zr, suggesting YDC had a full coverage on the YSZ sub surface.

In addition to Auger, we also employed an XPS surface scan analysis to inspect the extent of the YDC film coverage. Three samples were used for this purpose: SOFCs with 5×, 10× and 15× super cycles of YDC, respectively. One of the Zr main peaks is Zr-3d, which has a binding energy around 184 eV. By studying the intensities of the Zr-3d peaks of these samples, we determined whether the underlying YSZ substrate was fully covered and, therefore, whether a complete YDC film had been formed. High resolution scans within the binding energy regime ranging from 100 to 200 eV were performed on the above three samples, and their spectra were summarized in Fig. 4. During these XPS measurements, we employed a technique called angle resolved XPS. By tilting the sample stage of our XPS setup (10 ∼ 30°), we were able to limit the beam penetration depth to around 2 nm. That setup adjustment excluded signal interference from the detection of the underlying YSZ substrate. As the results show, 5 ALD super cycles were not enough to form a complete layer and the Zr-3d peak from the underlying YSZ electrolyte was detected. The Ce-4d peak was weak as well, indicating patchy YDC coverage. Ten ALD super cycles greatly improved the film coverage and Zr-3d peak was hardly distinguishable from the background. No Zr-3d peak was discernible under 15 ALD super cycles of YDC film. The XPS results show that the YDC thin film forms near-full coverage starting from 10 ALD super cycles.

The identified optimal YDC interlayer can be employed in various applications, with one area being micro fuel cells. When the electrolyte thickness is reduced to the sub micron scale, the thickness effects of the additional YDC layer cannot be ignored anymore. Inserting the YDC layer with the least-needed thickness can avoid increased ohmic losses and the associated performance drops. Fig. 5 is an illustration of the cross-sectional view of an YDC interlayered SOFC. Ten super cycles of ALD YDC was deposited on top of 100 super cycles of ALD YSZ to enhance the oxide ion

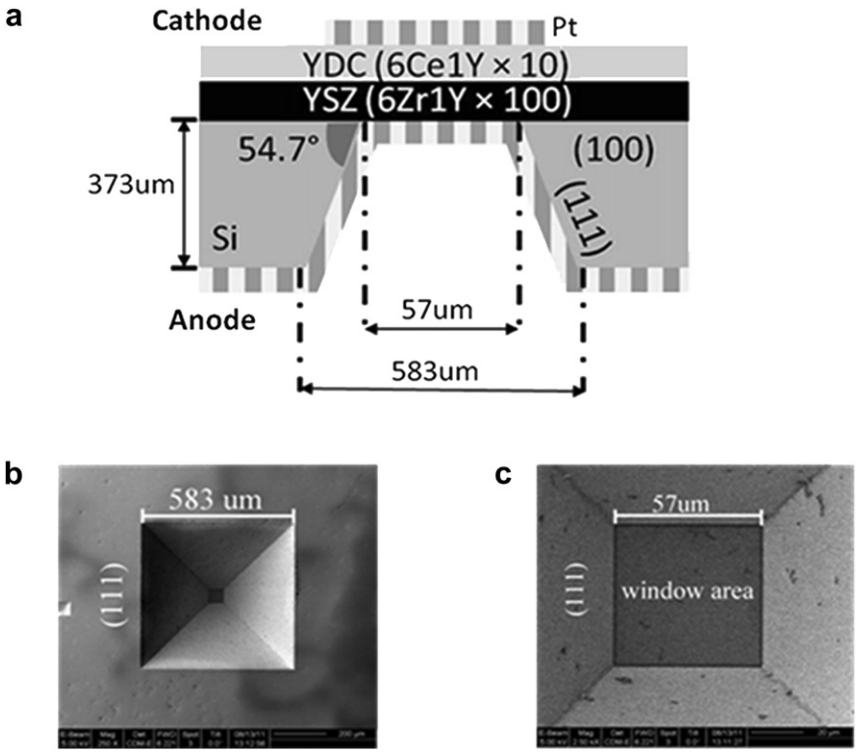

Fig. 5. (a) Illustration of YDC interlayered micro SOFC sample (not drawn to scale). Bulk YSZ electrolyte was fabricated via ALD recipe (6Zr: 1Y) × 100 and interlayered YDC was done via ALD recipe (6Ce: 1Y) × 10. (b, c) A freestanding individual fuel cell with an effective window size of (57 um)^2.

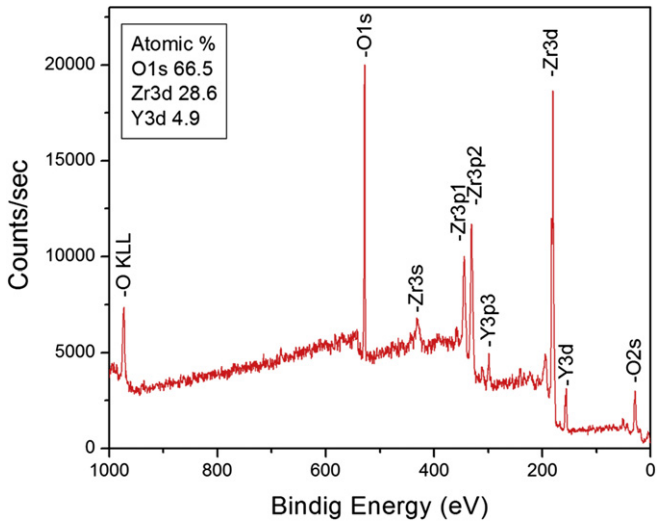

Fig. 6. XPS survey scan of the deposited ALD YSZ film. The ALD was done via a recipe of (6Zr: 1Y) × 100 and the resulting film has an 8 M% Y_2O_3 doping concentration.

incorporation kinetics at the cathode/electrolyte interface. YSZ electrolyte was fabricated by ALD with a recipe (6Zr:1Y) × 100. The resulting film was ≈70 nm with an 8 M % Y_2O_3 doping level. An XPS survey scan was performed on the deposited YSZ film and the desired stoichiometry was confirmed, as shown in Fig. 6. Porous Pt was deposited onto the YDC layer and the pattered anode-side. The open window is the effective area for fuel cell conduction and here it had a size of 57 um × 57 um, a value obtained through SEM imaging. For the purpose of comparison, a reference SOFC was also fabricated via a method similar to that described above, except that there was no YDC interlayer for the reference sample. The reference and YDC-interlayered samples were loaded in the customized fuel cell station sequentially and their IV performance was measured and analyzed. As shown in Fig. 7, P_{max} values for the reference SOFC

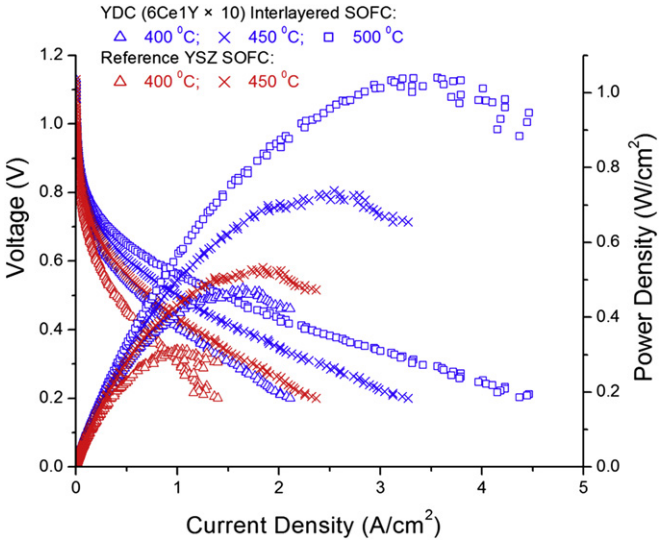

Fig. 7. Comparison of micro fuel cell performance of YDC interlayered sample (blue) and YSZ reference sample (red, micro fuel cells with YDC interlayering) at 400–500 °C. The effective window size is (57 um × 57 um). Both the cathode and anode are 80 nm porous Pt.(For interpretation of the references to color in this figure legend, the reader is referred to the web version of this article.)

were 0.31 and 0.53 W cm^{-2} at 400 and 450 °C, respectively, and 0.46 and 0.71 W cm^{-2} for the interlayered sample. Therefore, an average enhancement factor of 1.4 was achieved by inserting the YDC layer with the recipe (6Ce: 1Y) × 10. This YDC-interlayered SOFC was also tested at 500 °C, and a power density as high as 1.04 W cm^{-2} was obtained under the optimal experimental conditions. Here, the P_{max} enhancement factor of micro fuel cells was much lower than that of bulk fuel cells. One possible explanation was that the YDC film became partially contaminated during the backside Si_3N_4 layer removal via the reactive ion etching (RIE) process. Additional refinement of the fabrication procedure is needed to further enhance the performance of the micro fuel cells [20–22].

4. Conclusion

Thickness effects of the YDC interlayer were investigated. By comparing the *I–V* performance of bulk SOFCs with different numbers of ALD super cycles, we identified the optimal YDC recipe as (6Ce: 1Y) × 10. With the help of this interlayer, P_{max} was enhanced 2.5–3.7 times, at operating temperatures between 300 and 450 °C. Auger elemental mapping and XPS surface scans were consistent with our observations. This YDC interlayer has a wide array of applications, especially in the field of interface engineering. Micro fuel cells have an averaged 1.4× enhanced performance with this additive layer. Under the experimental conditions described here, a power density of 1.04 W cm^{-2} was achieved at 500 °C, which has the potential to be even further enhanced through more advanced cell fabrication techniques such as membrane corrugation.

Acknowledgment

The authors thank T. Gür and C.-C. Chao for helpful discussions on experimental analysis.

References

[1] S.M. Haile, Acta Materialia 51 (2003) 5981–6000.
[2] R.O.'. Hayre, S. Cha, W. Colella, F.B. Prinz, Fuel Cell Fundamentals, John Wiley and Sons, New York, 2006.
[3] A.J. McEvoy, Solid State Ionics 132 (2000) 159–165.
[4] N.P. Brandon, S. Skinner, B.C.H. Steele, Annu. Rev. Mater. Res. 33 (2003) 182–213.
[5] S.C. Singhal, K. Kendall, High Temperature Solid Oxide Fuel Cells: Fundamentals, Design and Applications, Elsevier, Oxford, UK, 2003.
[6] J.H. Shim, C.C. Chao, H. Huang, F.B. Prinz, Chem. Mater. 19 (2007) 3850–3854.
[7] T.P. Holme, R. Pornprasertsuk, F.B. Prinz, J. Electrochem. Soc. 157 (2010) B64–B70.
[8] B.C.H. Steele, K.M. Hori, S. Uchino, Solid State Ionics 135 (2000) 445–450.
[9] H. Huang, T. Holme, F.B. Prinz, J. Fuel Cell Sci. Tech. 7 (2010) 1–5.
[10] Z. Shao, S.M. Haile, Nature 431 (2004) 170–173.
[11] B.C.H. Steele, Solid State Ionics 75 (1995) 157–165.
[12] T. Mori, R. Buchanan, D.R. Ou, F. Ye, T. Kobayashi, J-D. Kim, J. Zou, J. Drennan, J. Solid State Electrochem. 12 (2008) 841–849.
[13] Z. Fan, C.C. Chao, F. Hossein-Babaei, F.B. Prinz, J. Mater. Chem. 21 (2011) 10903–10906.
[14] Z. Fan, F.B. Prinz, Nano Lett. 11 (2011) 2202–2205.
[15] M. Leskela, M. Ritala, Thin Solid Films 409 (2002) 138–146.
[16] O. Sneh, R.B. Clark-Phelps, A.R. Londergan, J. Winkler, T.E. Seidel, Thin Solid Films 402 (2002) 248–261.
[17] R.L. Puurunen, W. Vandervorst, J. Appl. Phys. 96 (2004) 7686–7695.
[18] N.P. Dasgupta, H.J. Jung, O. Trejo, M.T. McDowell, A. Hryciw, M. Brongersma, R. Sinclair, F.B. Prinz, Nano Lett. 11 (2011) 934–940.
[19] H. Huang, M. Nakamura, P. Su, R. Fasching, Y. Saito, F.B. Prinz, J. Electrochem. Soc. 154 (2007) B20–B24.
[20] C.C. Chao, C.M. Hsu, Y. Cui, F.B. Prinz, ACS Nano 5 (2011) 5692–5696.
[21] P.C. Su, C.C. Chao, J.H. Shim, R. Fasching, F.B. Prinz, Nano Lett. 8 (2008) 2289–2292.
[22] A. Evans, A. Bieberle-Hütter, J.L.M. Rupp, L.J. Gauckler, J. Power Sources 194 (2009) 119–129.